2011 American Control Conference
on O'Farrell Street, San Francisco, CA, USA
June 29 - July 01, 2011

The Development of AMR Sensors for Vehicle Position Estimation

S. Taghvaeeyan and R. Rajamani[1]

Abstract – **This paper focuses on the development of automotive sensors that can measure the relative position and velocity of another vehicle in close proximity, so as to enable prediction of an imminent collision just before the collision occurs. Anisotropic magnetoresistive (AMR) and sonar sensors are adopted for development of the proposed sensor system. The challenges in the use of the AMR sensors include their nonlinear behavior, limited range and magnetic signature levels that vary with each type of car. An adaptive filter based on the extended Kalman filter (EKF) is developed to automatically tune filter parameters for each encountered car and reliably estimate car position. The utilization of an additional sonar sensor during the initial detection of the encountered vehicle is shown to highly speed up the parameter convergence of the filter. Experimental results are presented from a large number of tests with various vehicles to show that the proposed sensor system is viable. The developed sensors represent perhaps the first ever system that can measure relative vehicle position at close proximity right up to the point where a crash occurs.**

1. INTRODUCTION

Research work in the case of predictive crash detection has mostly focused on the use of multiple radars and laser sensors (wide-beam short-range and narrow-beam long-range) for prediction of future collisions (see references [7], [8], [9], [10], [11]). However, such systems can only provide a probability of collision and cannot predict it with certainty. This is because the radar sensors used in such applications cannot make measurements at distances very close to the car (less than 1 meter) and have an extremely narrow field of view at such short distances. Hence these collision prediction systems are primarily useful for providing long-distance collision warnings to the driver, so that the driver can then respond and try to ensure a safe maneuver. Sometimes such collision prediction systems are also used to initiate automated gentle braking of the vehicle.

This paper aims to develop a reliable system for prediction of an imminent crash, a few tens of milli-seconds before the crash occurs. The development of such imminent collision detection systems will lead to smart deployment systems for seat belts and airbags, providing improved safety for passengers during a crash. Such crash detection systems can also be used in technologies that actively enhance vehicle crush space to mitigate the effects of the crash. For such applications (where airbags can be triggered based on collision warnings), a far more fool-proof and close-range collision detection system is needed than a system based on long range radar or laser sensors.

[1]Saber Taghvaeeyan and Rajesh Rajamani are with the University of Minnesota, Minneapolis, MN 55455, Email: rajamani@me.umn.edu, TEL 612-626-7961.

Funding for this research was partly provided by the ITS-Institute at the University of Minnesota.

For such collision detection, a sensor system that is inexpensive, continues to work at very close range values, has a wide field of view at short range and measures the other car's position and velocity just before collision is required. This will ensure that the collision detection system is both reliable and works over the entire required operating range.

A strong candidate for such a collision detection sensor is an anisotropic magneto-resistive (AMR) sensor. The use of AMR sensors for detection of vehicles in parking spots [12] and for measurement of traffic flow rate by embedding AMR sensors in the road ([12], [13]) have been previously studied. However, the use of AMR sensors for detection of imminent collision and for measurement of vehicle position and velocity has not been considered by researchers and has not been previously studied.

2. AMR SENSORS AND POSITION ESTIMATION

An AMR sensor has a silicon chip with a thick coating of piezoresistive nickel-iron. The presence of an automobile in close range causes a change in magnetic field which changes the resistance of the nickel-iron layer. The 3-axis HMC 1053 set of AMR devices from Honeywell were utilized for the system developed in this paper. Application note AN218 from Honeywell describes the use of the HMC 105X chips for vehicle detection and traffic counting applications (neither of which involves vehicle position estimation).

A number of tests with different vehicles were performed in order to investigate the magnetic field generated by an encountered vehicle as a function of distance. Figure 1 shows a general schematic of the preliminary tests. An AMR sensor and a sonar sensor were packaged on a PCB together with a microprocessor that read the sensor signals and transmitted their values to a computer.

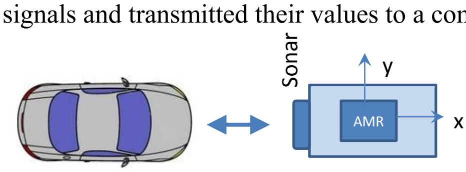

Figure 1: General scenario of the experiments

The outputs of the AMR and sonar sensors were sampled at the rate of 2 KHz using a dsPIC microcontroller with 12-bit ADC. Figure 2 shows the relationship between the magnetic field (in the X direction) and actual distance obtained from a sonar sensor for a typical test using a Chevy Impala vehicle. Magnetic field is plotted in arbitrary voltage units, the same as what was read from the ADC of the microcontroller. It can be seen that there is obviously a nonlinear relation between the measured magnetic field and distance.

The first step in order to check if AMR sensors can be used for distance measurements is to see if there is a reliable relation between magnetic field and vehicle distance. According to basic electromagnetic books [1], [2], the magnetic field created by a magnetic dipole can be obtained from the following equation.

$$B_{dip}(\boldsymbol{r}) = \frac{k}{r^3}(3(\boldsymbol{m}.\hat{\boldsymbol{r}})\hat{\boldsymbol{r}} - \boldsymbol{m}) \quad (1)$$

where k is a constant, $\boldsymbol{m}$ is the magnetic dipole moment and $\boldsymbol{r}$ is the vector from position of the dipole to the position of the point where the field is being measured. Using this equation, one would be able to obtain the magnetic field for different objects by applying appropriate integration, which in general results in an equation for the magnetic field having an inverse relation with distance and its higher orders. In our case, it was observed that below a threshold distance, x_{th}, the following relation can be assumed between magnetic field and distance

$$B = \frac{p}{x} + q \quad (2)$$

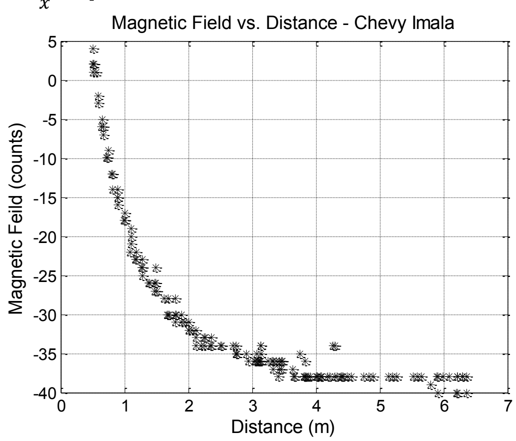

Figure 2: Result of the experiments with Chevy Impala showing magnetic field in X direction versus distance obtained from sonar sensor

where B is the magnetic field, x is distance of the vehicle from the sensors, p and q are vehicle dependent parameters. This equation was fit to experimental data from various vehicles. Figures 3 and 4 show the fitting results from two experiments with a Chevrolet Impala and a VW Passat. In both of the experiments, the vehicle was moved from an initial large distance toward the sensors. In these figures, data set 1 is the set of data points obtained after the vehicle gets closer than x_{th} to the sensors. This data set was used for curve fitting. Data set 2 is the set of data points from the same experiment where the vehicle was further than x_{th} from the sensors and is plotted for comparison. The equation was also verified against data from the same type of experiment with Hyundai Elantra and Honda Accord vehicles.

An estimate of x_{th} can be obtained even by visually inspecting the graphs or from the following fact that

$$\begin{cases} B = B_{stat} & x \geq x_{th} \\ B = \frac{p}{x_{th}} + q & x \leq x_{th} \end{cases} \quad (3)$$

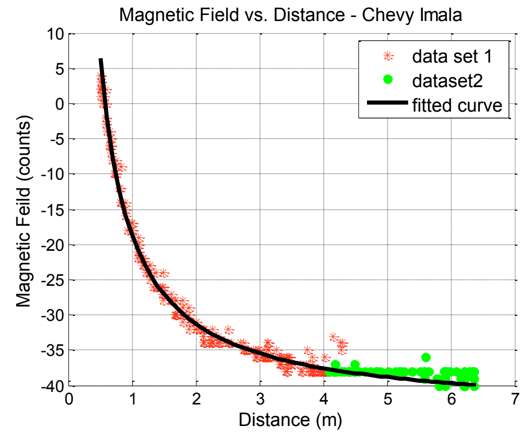

Figure 3: Result of the experiment with Chevy Impala and fitted curve

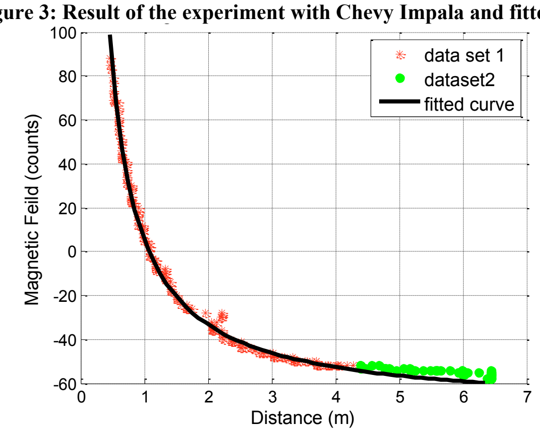

Figure 4: Result of the experiment with WV Passat and fitted curve

where B_{stat} is the static magnetic field measured by the AMR sensor when there is no vehicle close to it. Therefore, at $x = x_{th}$, we have

$$B_{stat} = \frac{p}{x_{th}} + q \quad (4)$$

One can obtain an estimate of x_{th} by the following equation

$$x_{th} = \frac{p}{B_{stat} - q + e} + q \quad (5)$$

where e is a positive constant used to ensure that the change in magnetic field is caused by the vehicle and not quantization error and noise. Table 1 summarizes the results of the experiments showing $R^2$of the fitted curve from equation (2) and estimated x_{th} for various vehicles.

Vehicle	p	$B_{stat} - q$	R^2	x_{th}
Chevy Impala	25.26	3.23	0.997	~4.8
Honda Accord	-28.42	-6.79	0.999	~3.2
WV Passat	74.38	14.38	0.997	~4.5
Hyundai Elantra	-10.2	-3.21	0.999	~3

Table 1: Results from curve fitting

Technical Challenges

The next step would be to adopt the proposed equation for close distance sensing. However, it is worth mentioning here that from different experiments, it was observed that the speed of the approaching vehicle has a slight but noticeable effect on measured magnetic field. This is shown in Figure

5. The offset in the magnetic field, B_{stat}, has been subtracted from the measured data so that the difference can be illustrated better. The same trend was also seen in experiments with the Chevy Impala and the Hyundai Elantra.

The magnetic field generated by the vehicle also changes with changing the global position and orientation of the experiment. One possible explanation for this is that some of the metal in the vehicle body is magnetized in the earth magnetic field and affects the total magnetic field seen by the sensors.

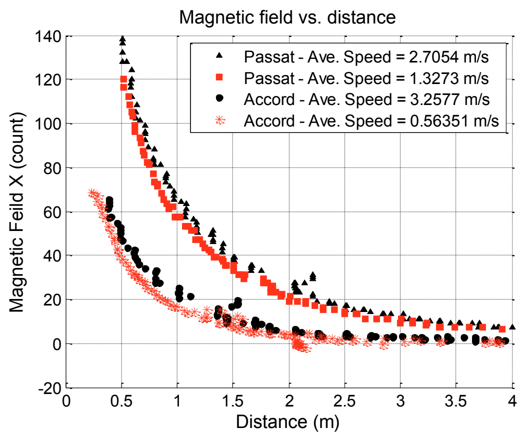

Figure 5: Effect of Speed on measured magnetic field

Furthermore, the values of the parameters p and q vary with the vehicle, being constant for a specific vehicle but changing from one vehicle model to another. Since the type of vehicle encountered is not known apriori, these parameters have to be adaptively updated in real-time.

3. ITERATED EXTENDED KALMAN FILTER (IEKF) FOR ADAPTIVE POSITION ESTIMATION

In the previous section we found a relation between distance and magnetic field. Knowing parameters p and q, one would be able to estimate the distance by using only the AMR sensor. However, these parameters change from one vehicle to another vehicle and from one location to another location. Therefore, the critical challenge would be to estimate p and q accurately and quickly in real time and use them to estimate the distance of the approaching vehicle from the sensors.

To address this challenge, the use of two AMR sensors located apart from each other by a distance d in the X-axis as shown in Figure 6, is used. The approaching vehicle is assumed to be close enough to affect both AMR sensors. The use of two sensors enables the estimation of both parameters p and q. The vehicle position can then be subsequently obtained. Figure 7 shows a PCB with two AMR sensors and one sonar sensor, with the dsPIC processor and other needed electronics.

We can write the following equations for the measured magnetic fields

$$\begin{cases} B_{1m}(t_k) = \frac{p}{x(t_k)} + q_1 + n_1 \\ B_{2m}(t_k) = \frac{p}{x(t_k)+d} + q_2 + n_2 \end{cases} \qquad (6)$$

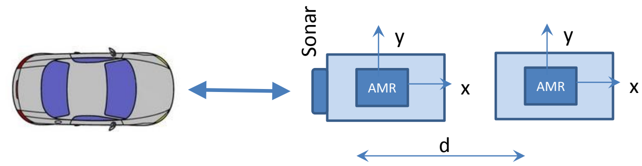

Figure 6: Experiments with two AMR sensors apart from each other by distance d

Figure 7: The developed PCB for experiments

where B_{1m} and B_{2m} are the measured magnetic fields and n_1 and n_2 are noise. It should be noted that q_1 and q_2 are not necessarily equal since B_{1stat} and B_{2stat} can be quite different. However considering the fact that x_{th} is the same for both of the equations, we can write the following equations

$$\begin{cases} B_{1stat} = \frac{p}{x_{th}} + q_1 \\ B_{2stat} = \frac{p}{x_{th}} + q_2 \end{cases} \Rightarrow q_2 = q_1 + \Delta B_{stat} \qquad (7)$$

where $\Delta B_{stat} = B_{2stat} - B1_{stat}$. If we eliminate x from equations (6) and drop the time index we will have

$$\begin{aligned} dB_1(B_2 - \Delta B_{stat}) &= \big(B_1 - (B_2 - \Delta B_{stat})\big)p \\ &+ d\big(B_1 + (B_2 - \Delta B_{stat})\big)q_1 - dq_1^2 \\ &+ \big(-p - dq_1 + d(B_2 - \Delta B_{stat})\big)n_1 \\ &+ (p + dB_1 - dq_1)n_2 - dn_1 n_2 \end{aligned} \qquad (8)$$

This equation can be used to estimate p and q_1 and then subsequently obtain an estimate x using equations (6). Among the various estimators, the IEKF [3], [4] was chosen as a reasonable option for this nonlinear estimation problem. It should be noted that since we are not considering the dynamic equations of the vehicle, there would be no time updates for IEKF, only measurement updates. It also worth mentioning that the ordinary UKF [5], [6] estimators fail in this case, mainly because of the discontinuity at $x = 0$.

Putting the above relation into IEKF equations the states and noise definitions are

$$X = [p\ q_1]', n = [n_1\ n_2]', n \sim (0, R)$$

and the measurement equation is

$$Z = h(X, n)$$

$$Z = dB_1(B_2 - \Delta B_{stat})$$

$$\begin{aligned} h(X,n) = &\ \big(B_1 - (B_2 - \Delta B_{stat})\big)p \\ &+ d\big(B_1 + (B_2 - \Delta B_{stat})\big)q_1 - dq_1^2 \\ &+ \big(-p - dq_1 + d(B_2 - \Delta B_{stat})\big)n_1 \\ &+ (p + dB_1 - dq_1)n_2 \\ &- dn_1 n_2 \end{aligned} \qquad (9)$$

The measurement update equations are as follows

$$H_k = \frac{\partial h_k}{\partial x}\bigg|_{\hat{X}_k^-} = [B_{1,k} - (B_{2,k} - \Delta B_{stat}) + d\left(B_{1,k} + (B_{2,k} - \Delta B_{stat})\right) - 2d\hat{q}_{1,k-1}] \tag{10}$$

$$M_k = \frac{\partial h_k}{\partial n}\bigg|_{\hat{X}_k^-} = [-\hat{p}_{k-1} - d\hat{q}_{1,k-1} + d(B_{2,k} - \Delta B_{stat})\,\hat{p}_{k-1} + dB_{1,k} - d\hat{q}_{1,k-1}]$$

$$K_k = P_{k-1}H_k^T(H_kP_{k-1}H_k^T + M_kR_kM_k^T)^{-1}$$
$$\hat{X}_k = \hat{X}_{k-1} + K_k[Z_k - h_k(\hat{X}_{k-1}, 0)]$$
$$P_k = (I - K_kH_k)P_{k-1} \tag{11}$$

Applying the estimator to data obtained from experiments we should be able to estimate p and q_1 and by using them we should get an estimate of distance. To verify this, more tests were performed in which the vehicle moved toward the sensors from an initial distance and sensor outputs were recorded. Then a portion of data in which, according to the sonar sensor, the vehicle was closer than x_{th} to the sensors was selected and the designed IEKF estimator was applied. The results are shown in Figure 8 and Figure 9.

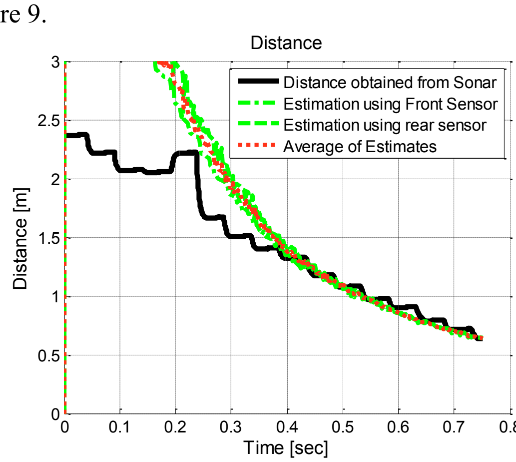

Figure 8: Distance obtained from sonar sensor and estimated distances

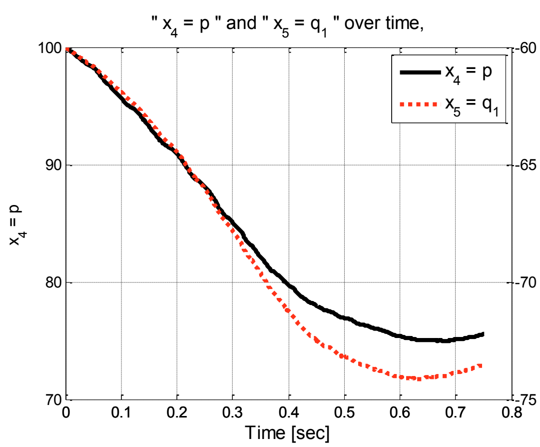

Figure 9: estimated *p* over time

It can be seen that the parameters p and q both converge in a period of about 0.6 seconds, as seen in Figure 9. The resulting position estimation as seen in Figure 8 also converges very well to the position measured by the sonar sensor.

4. SENSOR FUSION WITH SONAR FOR IMPROVED CONVERGENCE

The parameters p and q vary with the type of vehicle encountered. When the vehicle is first encountered, the value of the distance is likely to be large enough for a sonar sensor to work satisfactorily at that distance. A sonar sensor can directly measure position independent of vehicle size and independent of relative speed with respect to the sensor. It can measure larger distances of several feet compared to the AMR sensors but typically will not be able to work at very short distances below 1 or 2 feet. Furthermore, it has a narrow field of view at short distances.

A sensor fusion system can be used to exploit the advantages of both types of sensors to overcome their individual problems. Therefore a new architecture was designed for the estimator using the finite state machine shown in Figure 10. In state 0, the estimator will use the sonar sensor to update position, since the AMR sensors are not yet affected by the approaching vehicle. As soon as the AMR sensors respond to the approaching vehicle, updates would be done using both sonar and AMR sensors (state 1). When the vehicle enters a distance where the sonar readings are not valid any more due to very small distances, updates would be done using only the AMR sensors (state 2).

For transitions between the states in the finite state machine, x_{th} would be the best variable to utilize for switching from state 0 to 1, but there is no prior knowledge about x_{th} when a new vehicle is approaching. Therefore, the covariance of the AMR data at pre-determined time intervals can be used instead. Starting from state 0, whenever the covariance is higher than a threshold, the estimator switches to state 1 in order to switch from sonar to sonar-AMR updates. To obtain more meaningful initial values for the states p and q_1, a LS fitting can be done at the switching time. The estimated values and their covariance are used as initial values for p and q_1 and their covariance. While in state 1, x_{th} can be calculated in real-time and be used for determining if the vehicle is moving out of the view of the AMR sensors or the sonar sensor and if the system should switch back to state 0 or switch to state 2.

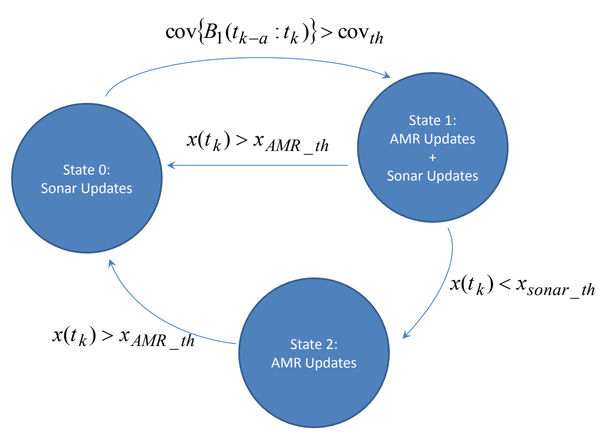

Figure 10: Architecture of the new estimator using sensor fusion

The next step is to develop the IEKF estimator equations for state 1 operation. The equations are presented below in the general case where the states would be updated with both sonar and AMR sensors. The system and measurement equations are given as follows

$$X_k = FX_{k-1} + Gw_{k-1}$$
$$Z = h(X,n)$$
$$w_k \sim (0, Q_k)$$
$$n_k \sim (0, R_k)$$

where

$$X = [x \quad v \quad a \quad p \quad q_1]^T$$

$$F = \begin{bmatrix} 1 & dt & 0 & 0 & 0 \\ 0 & 1 & dt & 0 & 0 \\ 0 & 0 & 1 & 0 & 0 \\ 0 & 0 & 0 & 1 & 0 \\ 0 & 0 & 0 & 0 & 1 \end{bmatrix}, G = \begin{bmatrix} 0 & 0 \\ 0 & 0 \\ 1 & 0 \\ 0 & 1 \\ 0 & 0 \end{bmatrix}$$

$$Z = [x_s \quad B_1 \quad (B_2 - \Delta B_{stat})]^T$$
$$n = [n_x \quad n_1 \quad n_2]^T$$
$$h(X,n) = \left[x + n_x \quad \frac{p}{x} + q_1 + n_1 \quad \frac{p}{x+d} + q_1 + n_2\right]^T$$

The time update equations would be as follows

$$\hat{X}_k^- = f_{k-1}(\hat{X}_{k-1}^+, u_{k-1}, 0)$$
$$P_k^- = FP_{k-1}^+F^T + GQ_{k-1}G^T$$

The measurement update equations would be as follows

$$K_k = P_k^- H_k^T (H_k P_k^- H_k^T + M_k R_k M_k^T)^{-1}$$
$$\hat{X}_k^+ = \hat{X}_k^- + K_k[Z_k - h_k(\hat{X}_k^-, 0)]$$
$$P_k^+ = (I - K_k H_k) P_k^-$$

where

$$H_k = \frac{\partial h_k}{\partial X}\bigg|_{\hat{X}_k^-} = \left.\begin{bmatrix} 1 & 0 & 0 & 0 & 0 \\ -\frac{p}{x^2} & 0 & 0 & \frac{1}{x} & 1 \\ -\frac{p}{(x+d)^2} & 0 & 0 & \frac{1}{x+d} & 1 \end{bmatrix}\right|_{\substack{x = \hat{x}_k^- \\ p = \hat{p}_k^- \\ q_1 = \hat{q}_{1,k}^-}} \tag{12}$$

$$M_k = \begin{bmatrix} 1 & 0 & 0 \\ 0 & 1 & 0 \\ 0 & 0 & 1 \end{bmatrix} \tag{13}$$

Now based on the value of the current state in the finite state machine, the appropriate updates can be performed. The estimator is then tested using experiments. The following experiments were performed to check the estimator. A VW Passat car approached the sensors and moved away (between 5 and 15 seconds), then a Chevrolet Impala came close to the sensors and moved away (between 20 and 30 seconds). The results are shown in figures 11 to 16. The red circles in these figures indicate the time at which a transition in the finite state machine occurred.

As can be seen from the figures, the proposed algorithm to switch between states in a finite state machine and get an initial value for p and q_1 works very well. Excellent estimation of distance is obtained as seen in Figure 12. This is inspite of the change in vehicles that occurs between the VW Passat and the Chevy Impala during the experiment. As seen in Figure 15, p converges quickly and changes in value between the two vehicles. Likewise the parameter q also changes in value between the two vehicles. It can be also seen that the final values of sonar distance and estimated distance in each scenario are not exactly the same. At this point it is not clear if this is due to the inaccuracy of sonar sensor or AMR estimation and needs to be considered further.

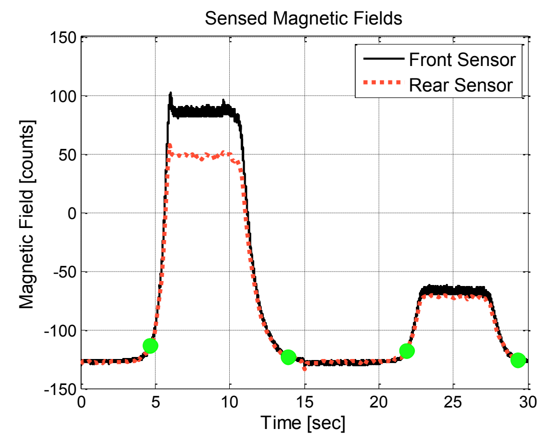

Figure 11: Sensed magnetic fields over time

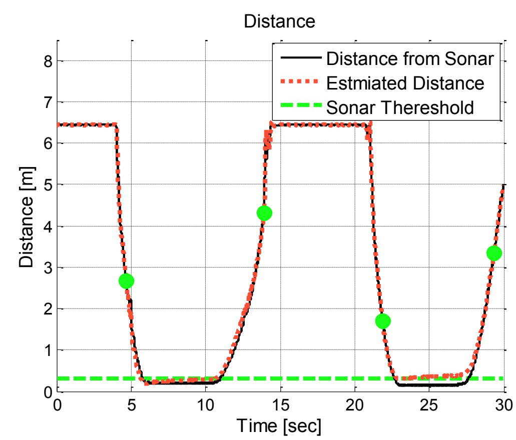

Figure 12: Distance obtained from sonar sensor, estimated distance and sonar threshold below which the sonar data is ignored

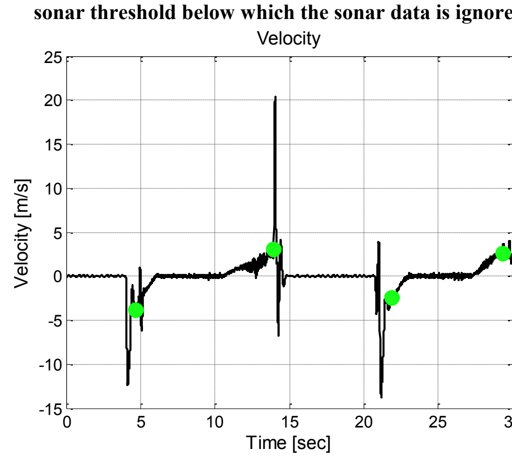

Figure 13: Estimated velocity

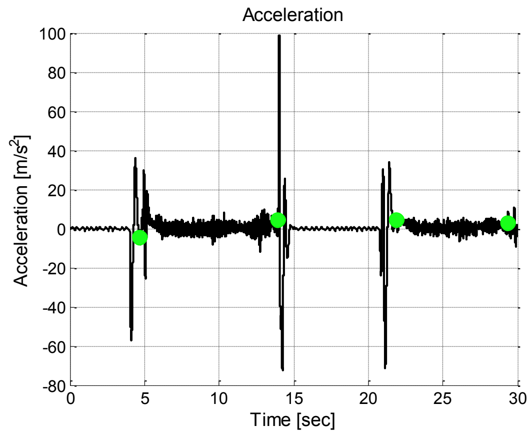

Figure 14: Estimated acceleration

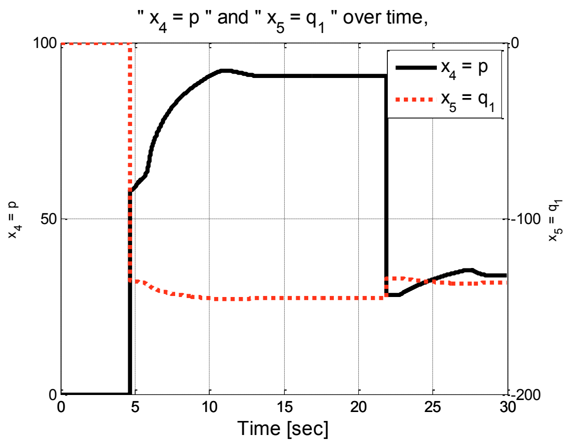

Figure 15: Estimated *p*

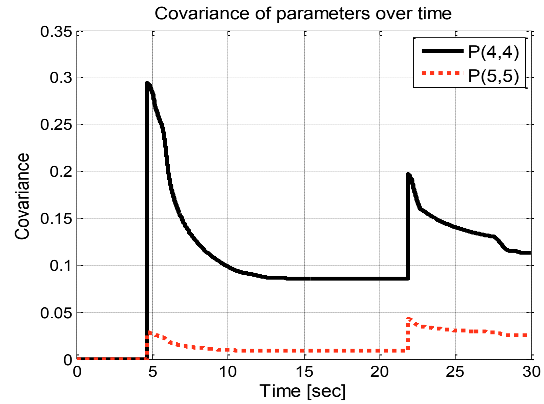

Figure 16: Covariance of *p* and *q*

5. CONCLUSIONS

This paper focuses on the development of automotive sensors that can measure the relative position and velocity of another vehicle in close proximity, so as to enable prediction of an imminent collision just before the collision occurs. Anisotropic magnetoresistive (AMR) and sonar sensors are adopted for development of the proposed sensor system. The challenges in the use of the AMR sensors include their nonlinear behavior, limited range and magnetic signature levels that vary with each type of car. An adaptive filter based on the iterated extended Kalman filter (IEKF) is developed to automatically tune filter parameters for each encountered car and reliably estimate car position. The usage of an additional sonar sensor during the initial detection of the encountered vehicle is shown to highly speed up the parameter convergence of the filter. Experimental results are presented from tests with a large number of various vehicles to show that the proposed sensor system is viable. The developed sensors represent perhaps the first ever system that can measure relative vehicle position at close proximity right up to the point where a crash occurs. The results in this paper have shown that it is possible to have an adaptive estimator that can adapt to the AMR sensor parameters which are dependent on the specific vehicle encountered.

References

[1] H. Knoepfel, *Magnetic Fields : A Comprehensive Theoretical Treatise for Practical use.* Wiley, 2000.

[2] David J. Griffiths, *Introduction to Electrodynamics.* Prentice Hall, 1999.

[3] Y. Bar-Shalom, X. Rong Li, T. Kirubarajan, *Estimation with Applications to Tracking and Navigation.* Wiley, 2001.

[4] D. Simon, *Optimal State Estimation: Kalman, H Infinity, and Nonlinear Approaches.* Wiley, 2006.

[5] S. Julier, J. Uhlmann and H. F. Durrant-Whyte, "A new method for the nonlinear transformation of means and covariances in filters and estimators," *Automatic Control, IEEE Transactions on,* vol. 45, pp. 477-482, 2000.

[6] T. Lefebvre, H. Bruyninckx and J. De Schuller, "Comment on "A new method for the nonlinear transformation of means and covariances in filters and estimators" [and authors' reply]," *Automatic Control, IEEE Transactions on,* vol. 47, pp. 1406-1409, 2002.

[7] R. Mobus, U. Kolbe, "Multi-target multi-object tracking, sensor fusion of radar and infrared," IEEE Intelligent Vehicles Symposium, Volume, 14-17 June 2004, pp. 732 – 737

[8] S. Matzka and R. Altendorfer, "A Comparison of Track-to-Track Fusion Algorithms for Automotive Sensor Fusion," Proceedings of IEEE International Conference on Multisensor Fusion and Integration for Intelligent Systems, Seoul, Korea, August 20 - 22, 2008.

[9] G. R. Widmann, M. K. Daniels, L. Hamilton, L. Humm, B. Riley, J. K. Schiffmann, D. E. Schnelker and W. H. Wishon, "Comparison of Lidar-Based and Radar-Based Adaptive Cruise Control Systems," Delphi Automotive Systems, 2000-01-0345

[10] M.I. Ki, K. Yi, D. Caveney, J.K. Hedrick, "A multi-target tracking algorithm for application to adaptive cruise control," Journal of mechanical science and technology, 2005, vol. 19, no. 9, pp. 1742-1752

[11] D. Caveney, B. Feldman, and J.K. Hedrick, "Comprehensive Framework for Multisensor Multi-target Tracking in the Adaptive Cruise Control Environment," Proc. of the 6th International Symposium on Advanced Vehicle Control (AVEC), Hiroshima, Japan. Sept. 2002, pp. 697-702.

[12] M. H. Kang, B. W. Choi, K. C. Koh, J. H. Lees, G. T. Park, "Experimental study of a vehicle detector with an AMR sensor," Sensors and actuators. A, Physical, 2005, vol. 118, no. 2, pp. 278-284

[13] J. Vcelak, P. Ripka, J. Kubik, A. Platil and P. Kaspar, "AMR navigation systems and methods of their calibration,"Sensors and Actuators A: Physical, Vol 123-124, 23 September 2005, pp. 122-128.